Mesoporous Polymer Nanofibers by Infiltration of Block Copolymers with Sacrificial Domains into Porous Alumina

Yong Wang,* Ulrich Gösele, and Martin Steinhart*

Max Planck Institute of Microstructure Physics, Weinberg 2, 06120 Halle, Germany

Received November 1, 2007
Revised Manuscript Received December 5, 2007

An emerging approach toward the integration of mesoporous materials into functional device architectures is based on the self-assembly of amphiphilic block copolymers (BCPs) inside hard templates containing arrays of aligned cylindrical nanochannels.[1–6] The morphology defined by the soft template is fixated by cross-linking precursors for silica or amorphous carbon after their selective segregation to the hydrophilic domains. After gelation, organic components are removed by calcination, and mesoporous fibers consisting of silica[1–5] or amorphous carbon[6] are obtained. However, solvent evaporation and high-temperature calcination lead to substantial volume shrinkage. The resulting inhomogeneous filling of the hard templates with the mesoporous scaffold is a serious drawback for any application requiring mechanically stable membranes with uniform mesopore structure.

We report the fabrication of mesoporous polymer nanofibers by direct infiltration of microphase-separated BCP melts[7,8] into self-ordered anodic aluminum oxide (AAO)[9,10] and the subsequent removal of sacrificial domains from the nanofibers vitrified upon cooling. This approach yields AAO hybrid membranes containing a mesoporous polymeric scaffold and is therefore, to some extent, complementary to the preparation of nanotubes by the self-assembly of amphiphilic BCPs in solution.[11,12] For a proof of concept, we selected poly(styrene-*block*-methyl methacrylate), PS-*b*-PMMA, because the selective degradation of the PMMA domains in thin film configurations by exposure to UV light and subsequent rinsing with acetic acid has been proven to be an easy and reliable pathway to ordered nanoporous PS films.[13] It is reasonable to assume that liquid BCP soft templates confined to AAO hard templates undergo a significantly lower volume shrinkage upon cooling and vitrification than sol/gel systems during gelation and calcination. On the basis of the temperature dependence of the specific volume of PS reported in the literature,[14] we estimate the thermal shrinkage of the BCP nanofibers to be about 8% for the protocol described below. However, optimizing the procedure for their preparation in this regard may result in further reduction of the volume shrinkage down to a few percent.

The PS-*b*-PMMA was placed on top of AAO hard templates at a temperature of 220 °C and, driven by capillary forces, infiltrated according to protocols reported elsewhere.[16] The AAO hard templates had a pore depth of 100 μm and closed pore bottoms (the porous alumina layer was attached to an underlying aluminum substrate). The portion of the pores filled with the BCP is proportional to the square root of the infiltration time[15] and can easily be controlled.[7,16] For the proof of concept reported here, however, we selected protocols that led to the complete filling of the pores, as evidenced by scanning electron microscopy (SEM) investigations of cleaved AAO hard templates after their infiltation (see the Supporting Information, Figure S1). The samples were kept at 220 °C for 48 h and then cooled to room temperature at a rate of 1 K/min.[17] The residual BCP on the surface of the AAOs was scraped off with sharp blades. Subsequently, the PMMA was removed by UV irradiation and extraction of the degradation products with acetic acid.[18] We used PS-*b*-PMMA consisting of PS blocks with a number-average molecular weight M_n = 26 800 g/mol and PMMA blocks with M_n = 12 200 g/mol (Polymer Source Inc., Canada; the polydispersity indices of the PS blocks and the PS-*b*-PMMA were 1.02 and 1.07, respectively) with a bicontinuous bulk microphase structure,[19,20] to fabricate fibers combining high porosity and mechanical stability. A SEM[21] image of the surface of an AAO hard template with

* Corresponding author. E-mail: steinhart@mpi-halle.de (M.S.); yongwang@mpi-halle.de.

(1) Yang, Z.; Niu, Z.; Cao, X.; Yang, Z.; Lu, Y.; Hu, Z.; Han, C. C. *Angew. Chem., Int. Ed.* **2003**, *42*, 4201–4203.
(2) Lu, Q.; Gao, F.; Komarneni, S.; Chan, M.; Mallouk, T. E. *J. Am. Chem. Soc.* **2004**, *126*, 8650–8651.
(3) Wu, Y.; Cheng, G.; Katsov, K.; Sides, S. W.; Wang, J.; Tang, J.; Fredrickson, G. H.; Moskovits, M.; Stucky, G. D. *Nat. Mater.* **2004**, *3*, 816–822.
(4) Chen, X.; Steinhart, M.; Hess, C.; Gösele, U. *Adv. Mater.* **2006**, *18*, 2153–2156.
(5) Chen, X.; Knez, M.; Berger, A.; Nielsch, K.; Gösele, U.; Steinhart, M *Angew. Chem., Int. Ed.* **2007**, *46*, 6829–6832.
(6) Steinhart, M.; Liang, C. D.; Lynn, G. W.; Gösele, U.; Dai, S. *Chem. Mater.* **2007**, *19*, 2383.
(7) Xiang, H. Q.; Shin, K.; Kim, T.; Moon, S. I.; McCarthy, T. J.; Russell, T. P. *Macromolecules* **2004**, *37*, 5660.
(8) Sun, Y.; Steinhart, M.; Zschech, D.; Adhikari, R.; Michler, G. H.; Gösele, U. *Macromol. Rapid Commun.* **2005**, *26*, 369.
(9) Masuda, H.; Fukuda, K. *Science* **1995**, *268*, 1466–1468.
(10) Masuda, H.; Yada, K.; Osaka, A. *Jpn. J. Appl. Phys., Part 2* **1998**, *37*, L1340–L1342.
(11) Stewart, S.; Liu, G. *Angew. Chem., Int. Ed.* **2000**, *39*, 340–344.
(12) Shimizu, T.; Masuda, M.; Minamikawa, H. *Chem. Rev.* **2005**, *105*, 1401–1443.
(13) Thurn-Albrecht, T.; Steiner, R.; DeRouchey, J.; Stafford, C. M.; Huang, E.; Bal, M.; Tuominen, M.; Hawker, C. J.; Russell, T. P. *Adv. Mater.* **2000**, *12*, 787–791.
(14) Bohlen, J.; Kirchheim, R. *Macromolecules* **2001**, *34*, 4210–4215.
(15) Kim, E.; Xia, Y.; Whitesides, G. M. *Nature* **1995**, *376*, 581.
(16) Kriha, O.; Zhao, L.; Pippel, E.; Gösele, U.; Wehrspohn, R. B.; Wendorff, J. H.; Steinhart, M.; Greiner, A. *Adv. Funct. Mater.* **2007**, *17*, 1327–1332.
(17) The sample shown in Figure 2f had been kept for 24 h at 220°C before it was cooled to room temperature. However, we could not substantiate a systematic dependence of the morphology type on the annealing time that was varied between 10 and 48 h.
(18) The samples were irradiated with UV light for 30 min, using a 254 nm UV bench lamp (XX-15S, UVP, Inc; only one of the two available tubes was used to reduce the irradiation strength). Typically, the samples were then kept in acetic acid for 12 h.
(19) Hajduk, D.; Harper, P.; Gruner, S.; Honeker, C.; Kim, G.; Thomas, E.; Fetters, L. *Macromolecules* **1994**, *27*, 4063–4075.
(20) Förster, S.; Khandpur, A. K.; Zhao, J.; Bates, F. S.; Hamley, I. W.; Ryan, A. J.; Bras, W. *Macromolecules* **1994**, *27*, 6922–6935.

10.1021/cm703126r CCC: $40.75
Published on Web 12/22/2007

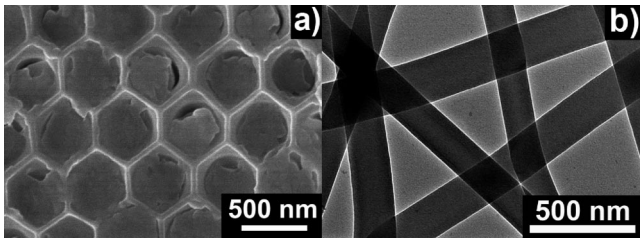

Figure 1. Electron microscopy images of native PS-*b*-PMMA nanofibers with a mean diameter of 200 nm prior to the removal of the PMMA. (a) SEM image of the surface of an AAO hard template infiltrated with the BCP; (b) TEM image of released native PS-*b*-PMMA nanofibers.

a lattice constant of 500 nm and a mean pore diameter of ~200 nm after the infiltration of the BCP is seen in Figure 1a and a transmission electron microscopy (TEM) image of PS-*b*-PMMA nanofibers released by etching the AAO template with aqueous KOH solution in Figure 1b.[22] It is obvious that prior to the selective removal of the PMMA, the PS-*b*-PMMA nanofibers are solid and do not show any indication of a mesopore structure.

After the selective removal of the PMMA, the residual PS nanofibers had a mesoporous fine structure with a mesh size of about 15−25 nm. A SEM image of the surface of an AAO hard template containing mesoporous PS nanofibers is displayed in Figure 2a. Their bicontinuous morphology is obvious from a SEM image showing the tips of PS nanofibers protruding from an AAO hard template whose uppermost layer was removed by dipping the sample into KOH solution (Figure 2b). SEM investigations of cross-sectional specimens prepared by cleaving AAO hard templates containing mesoporous PS nanofibers revealed that the PMMA could be removed completely over the entire depth of the AAO hard templates (Figure 2c and the Supporting Information, Figure S1).

The presence of selective surfaces influences the microphase separation in block copolymers[23–25] and can induce a lamellar phase in the proximity of the surface even if a BCP has a hexagonal bulk morphology.[26] TEM investigations revealed that the mesoporous PS nanofibers possessed an outermost, continuous PS layer with an apparent diameter of ~17 nm, which is indicative of surface-induced ordering. Besides a single-layer PS shell, the mesoporous nanofiber seen in Figure 2d with a diameter of ~385 nm exhibits a bicontinuous core morphology. In mesoporous nanofibers with smaller diameters, the competition between the bicontinuous core and the layered shell is obvious. In the mesoporous PS nanofibers shown in Figure 2e with a diameter of ~235 nm, a second and in some segments even a third layer parallel to the pore walls of the hard template

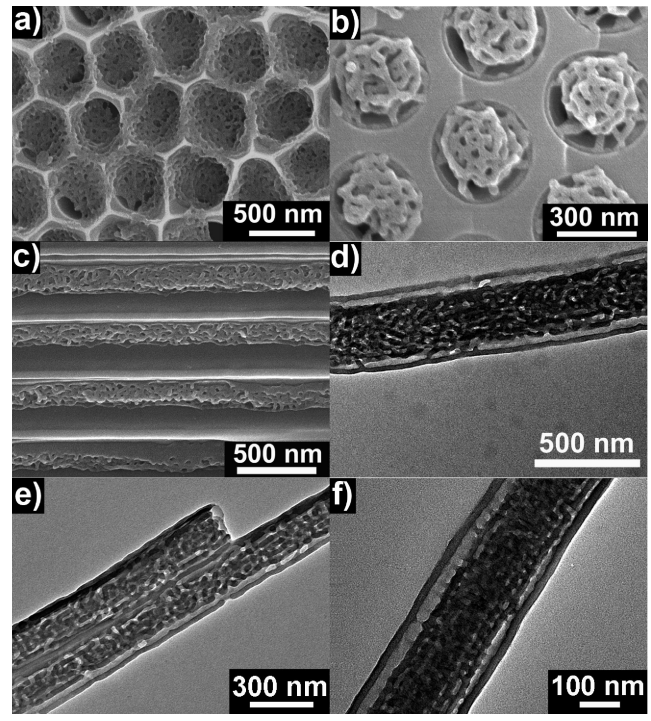

Figure 2. SEM and TEM images of mesoporous PS nanofibers after the selective removal of the PMMA. (a) SEM image of the surface of an AAO hard template containing mesoporous PS nanofibers. (b) SEM image of released tips of mesoporous PS nanofibers after the uppermost layer of the AAO hard template had been etched. (c) Cross-sectional SEM image of an AAO hard template cleaved along the pore axes containing mesoporous PS nanofibers. (d−f) TEM images of released mesoporous PS nanofibers with diameters of (d) 385, (e) 235, and (f) 250 nm. The morphology type seen in (d) and (e) was dominant; the perforated layer morphology seen in (f) occurred occasionally.

is seen. However, the layered structure is increasingly disturbed toward the fiber cores. Occasionally, the morphology type seen in Figure 2f occurred that is reminiscent of the hexagonally perforated layer structure[20,27–30] reported by Park et al. in thin films consisting of PS-*b*-PMMA with a similar block length ratio in the vicinity of smooth substrates.[31] The diameter of the mesoporous PS nanofiber shown in Figure 2f is ~250 nm.

It appears that the obtained morphologies result from a delicate competition between the surface-induced formation of a lamellar structure and the formation of tripod units of the minority component, which are characteristic of the bicontinuous bulk morphology of the BCP used, in the center of the PS-*b*-PMMA nanofibers. The interplay of these two incommensurate structural motifs induces to some extent disorder. However, the sharp size distributions of the mesopores in BCP-derived nanofibers rather than long-range-ordered domains are crucial to real-life applications of mesoporous membranes, such as separation.

(21) The samples were coated with a thin layer of Au/Pd alloy and probed with a JEOL JSM 6340F SEM operated at 10 keV.
(22) Suspensions of released nanofibers were dropped onto TEM grids coated with a holey carbon film and probed with a JEOL 1010 TEM operated at 100 keV.
(23) Fredrickson, G. H. *Macromolecules* **1987**, *20*, 2535–2542.
(24) Henkee, C. S.; Thomas, E. L.; Fetters, L. J. *J. Mater. Sci.* **1988**, *23*, 1685–1694.
(25) Coulon, G.; Russell, T. P.; Deline, V. R.; Green, P. F. *Macromolecules* **1989**, *22*, 2581–2589.
(26) Turner, M.; Rubinstein, M.; Marques, C. *Macromolecules* **1994**, *27*, 4986–4992.
(27) Hamley, I. W.; Koppi, K. A.; Rosedale, J. H.; Bates, F. S.; Almdal, K.; Mortensen, K. *Macromolecules* **1993**, *26*, 5959–5970.
(28) Hajduk, D. A.; Takenouchi, H.; Hillmyer, M. A.; Bates, F. S.; Vigild, M. E.; Almdal, K. *Macromolecules* **1997**, *30*, 3788–3795.
(29) Hajduk, D. A.; Ho, R. M.; Hillmyer, M. A.; Bates, F. S.; Almdal, K. *J. Phys. Chem. B* **1998**, *102*, 1356–1363.
(30) Vigild, M. E.; Almdal, K.; Mortensen, K.; Hamley, I. W.; Fairclough, J. P. A.; Ryan, A. J. *Macromolecules* **1998**, *31*, 5702–5716.
(31) Park, I.; Park, S.; Park, H. W.; Chang, T.; Yang, H. C.; Ryu, C. Y. *Macromolecules* **2006**, *39*, 315–318.

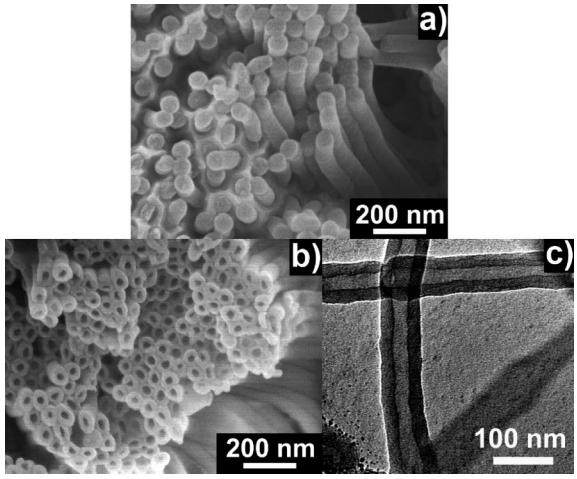

Figure 3. SEM and TEM images of nanofibers obtained from AAO templates with a mean pore diameter of 60 nm. (a) SEM image of native PS-*b*-PMMA nanofibers protruding from a partially etched AAO hard template; (b) SEM image of PS nanotubes after the selective removal of the PMMA domains that protrude from a partially etched AAO hard template; (c) TEM image of completely released PS nanotubes.

In hard templates with pore diameters on the same order of magnitude as the period of the infiltrated BCP, the influence of the pore walls and the geometric confinement cause the formation of microdomain morphologies fundamentally different from their bulk counterparts.[3,5,6,32–36] Infiltration of PS-*b*-PMMA into AAO with a mean pore diameter of 60 nm initially yields solid nanofibers without any obvious mesoporous structure (Figure 3a). However, after the removal of the PMMA blocks, PS nanotubes were obtained, arrays of which protruding from a partially etched AAO hard template are displayed in Figure 3b. TEM investigations revealed that the PS nanotubes indeed consist of only one PS shell with an apparent thickness of about 18 nm, whereas no features reminiscent of the bulk bicontinuous morphology were found (Figure 3c). Therefore, the self-assembly of the PS-*b*-PMMA is completely governed by surface-induced ordering.

In conclusion, the selective removal of a sacrificial constituent from BCP soft templates confined to AAO hard templates allows easy access to mesoporous polymer nanofibers that should be applicable to any BCP with a selectively degradable block, such as poly(ethylene oxide) or poly(lactide).[37] The hybrid membranes thus obtained are a promising material platform for applications in the fields of separation and filtration. As predicted theoretically, an ample body of microphase structures can be realized by confining BCPs to nanopores.[34] Thus, it should be possible to rationally design the morphology of the mesoporous BCP nanofibers by using BCP templates having specific molecular weights and compositions, and by engineering the interactions between the hard template and the constituents of the BCP. Because the pore walls of hard templates such as AAO can easily be modified by means of coupling agents such as silanes, they can be regarded as model interfaces for systematic studies of surface-induced ordering in BCPs. To this end, mesoporous nanofibers, which can easily be investigated by SEM and TEM, are ideal model systems.

Acknowledgment. Financial support by the German Research Foundation (SPP 1165 "Nanowires and Nanotubes") and the Volkswagen Foundation (Az. I/80 780), as well as technical support by K. Sklarek and S. Kallaus are gratefully acknowledged. Y. W. thanks the Alexander von Humboldt foundation for a fellowship.

Supporting Information Available: Large-field SEM images of cleaved AAO hard templates after their infiltration with PS-b-PMMA and the selective removal of the PMMA domains (PDF). This information is available free of charge via the Internet at http://pubs.acs.org.

CM703126R

(32) Shin, K.; Xiang, H. Q.; Moon, S. I.; Kim, T.; McCarthy, T. J.; Russell, T. P. *Science* **2004**, *306*, 76.
(33) Xiang, H.; Shin, K.; Kim, T.; Moon, S. I.; McCarthy, T. J.; Russell, T. P. *Macromolecules* **2005**, *38*, 1055–1056.
(34) Yu, B.; Sun, P.; Chen, T.; Jin, Q.; Ding, D.; Li, B. *Phys. Rev. Lett.* **2006**, *96*, 138306.
(35) Li, W.; Wickham, R. A.; Garbary, R. A. *Macromolecules* **2006**, *39*, 806–811.
(36) Chen, P.; Liang, H.; Shi, A.-C. *Macromolecules* **2007**, *40*, 7329–7335.
(37) Zalusky, A. S.; Olayo-Valles, R.; Wolf, J. H.; Hillmyer, M. A. *J. Am. Chem. Soc.* **2002**, *124*, 12761–12773.